Report of the Short Term Scientific Mission: "Brewer measurements in the visible range" (ES1207-17392)

H. Diémoz[1,2]

[1]ARPA Valle d'Aosta, Saint-Christophe, Italy
[2]Department of Physics, Sapienza – Univ. Roma, Roma, Italy

June 3, 2014

1 Purpose of the STSM

The capabilities of the Brewer spectrophotometers measuring in the visible range (MKIV) are largely underrated and underused. Yet, about 60 MKIV Brewers are operated worldwide, potentially providing an extended and useful dataset of aerosol optical depths (AODs) in the visible, at wavelengths of about 440 nm, and nitrogen dioxide (NO_2) vertical density columns (VCDs). The purpose of the STSM (May 5–16, 2014) is to bring this subject to the attention of the Brewer users community and to give new life to the Brewer visible products. A fundamental task is to compare the Brewer estimates to other reference instruments (ground based and satellites) and to state the capabilities and limitations of MKIV instruments.

The Academy of Athens has been operating a MKIV Brewer (#001) since 2004 on the roof of the Biomedical Research Foundation (38.0°N, 23.8°E, 190 m asl). The campus is located in a green area at a distance of about 4 km from the centre of the city and it is thus partly influenced by urban emissions. The latter, which have been studied in recent works (Vrekoussis et al., 2013), show large descending trends due the economic recession in the last few years, which should be clearly identified by every ground-based instrument. Therefore, the NO_2 series recorded by Brewer #001 is particularly interesting to analyse. However, in my previous work (Diémoz, 2014), I reported about several issues concerning the Brewer measurements at this station, the most problematic being the wavelength dependence of the NO_2 estimates on small micrometer misalignments. The issue was temporarily overcome by applying a "piecewise" calibration on the various portions of the series using the bootstrap method described by Herman et al. (2009), which has however the effect of smoothing every seasonal cycle and climatological trend. Moreover, the correlation between the Brewer and spaceborne radiometers (OMI, SCHIAMACHY, GOME2) was observed to be generally rather low (with maximum correlation index 0.48). This STSM is thus a good chance to develop a different approach to solve the issues concerning the NO_2 retrieval and to throw some light on the discrepancies between the Brewer and the satellite estimates.

Additionally, a Cimel photometer is installed at the same location since 2008 (Fig. 1). The instrument is operating within the AERONET network (Holben et al., 1998), which soared, among others, to the reference aerosol network. A complex processing, consisting of progressive levels of accuracy, has been set up by AERONET, which ensures the maximum data quality. Since one of the short-band channels of the Cimel is centred at about 440 nm, the AOD retrieved by the Brewer and the sun photometer can be effectively compared. Since both instruments (Brewer MKIV and Cimel) operate in Athens at the same site, and since favourable weather conditions occur generally in the area, the Athens station seemed to be the perfect choice for a STSM.

This short report is a first and quick description of the work carried out during the STSM and does not pretend to be exhaustive or rigorous as a real publication. The first part is focussed on the AOD

Figure 1: The MKIV Brewer #001 spectrophotometer and the Cimel sun/sky photometer on the roof of the Biomedical Research Foundation.

while the second on nitrogen dioxide.

2 Aerosol optical depth

2.1 Method and algorithm

Since the purpose of this part of the work is to investigate about the maximum accuracy attainable by the Brewer and the Athens station can rely on an already validated reference instrument, the Brewer has not been considered as a "standalone" instrument, such as in other published works on the same subject (e.g., Gröbner and Meleti, 2004; Cheymol and De Backer, 2003). Therefore, I haven't focussed on the Langley calibration or on cloud-screening algorithms based on the Brewer alone, but rather I transferred the Cimel calibration to the Brewer and I compared the data measured nearly simultaneously by both instruments. As a consequence, the AERONET cloudscreening procedures (Smirnov et al., 2000) should guarantee an effective removal of the cloud interferences from the Brewer measurements as well. 787 measurements from the Brewer and the Cimel meet the acceptance criteria and will be used in the following analysis.

The direct sun series obtained by the Brewer are processed using an algorithm expressly developed for the STSM, taking into account all known factors affecting the measurements:

1. the traditional data reduction – consisting in the subtraction of the dark counts, the count rates calculations from raw counts and the dead time compensation – is applied as usual;

2. the count rates are compensated taking into account the spectral attenuations by the neutral density filters in the visible range;

3. unlike the AOD algorithm in the Brewer operating software, the Earth-Sun distance is now included in the data processing;

4. the count rates are compensated for the effects of the internal polarisation (Cede et al., 2006), mainly owing to the quartz window and the diffraction grating. The method is based on the theoretical formula (method 1) described in the paper, since no experimental characterisation of such an effect for Brewer #001 was available at the moment of the mission;

5. although a slight temperature dependence is visible from accurate analysis and will be described further in the text (Sect. 2.6), no relevant improvements have been obtained by applying a temperature correction. For this reason, no correction is applied at the moment;

6. in order to adopt a processing scheme as similar as possible to the one used by AERONET, the solar zenith angle and the aerosol air mass factor (AMF) are calculated using the formulae by Michalsky (1988) and Kasten and Young (1989), respectively. Refraction is included in the calculation. All results have been carefully checked against the ancillary outputs of the AERONET algorithm;

7. for the same reason, the Rayleigh optical depth is calculated using Bodhaine et al. (1999) coefficients, as in the AERONET algorithm. For the Rayleigh calculations, the same atmospheric pressure as given to the AERONET algorithm is also considered for the Brewer;

8. the NO_2 climatology used by AERONET for the Athens station is also used to process the Brewer data and remove the NO_2 contribution from the AOD.

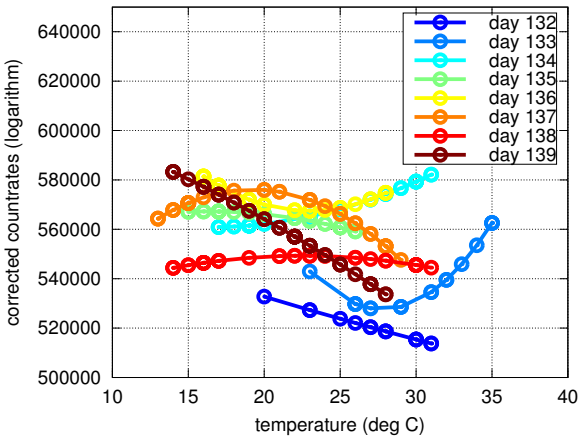

Figure 2: Corrected count rates from the third slit registered during `n2sl` tests as a function of the instrumental temperature. The curves represent a second order fit to all points.

The Bouguer-Langley-Beer law (Bouguer, 1729) is then used to retrieve the AOD from the corrected count rates.

The implementation of the algorithm is performed in two steps. A first script, written in Perl and called `bform.pl` - along the lines of `dsform.f` in the sunrad suite (Estellés et al., 2012) -, translates the raw data recorded in the Brewer B-files to a matrix, easily readable by any software. Then, an Octave/Matlab program is used to process the data. The software is written in a vectorised form and is thus very fast. A copy of `bform.pl` and some useful routines are freely available to the Brewer users community at the link: `www.arpa.vda.it/download/aod440_20140530.zip`.

2.2 Preliminary tests

Some tests were included in the Brewer schedule several weeks before the STSM to collect as many data as possible to accurately characterise the instrument. The spectral attenuation of the neutral density filters has been measured in the visible through a modified `fi` routine (the routine traditionally used in the `o3` mode does not work in `n2` mode), running every night, in the first days, and then on a weekly basis.

Also, a special schedule including a large number of `n2ds` (direct sun measurements in the visible) has been developed and used during the STSM, and some weeks after, to gather and process as many direct sun measurements as possible.

Table 1: Wavelengths (in nm) and resolutions (Full Widths at Half Maximum in nm) for every slit of Brewer #001.

slit	wavelength (nm)	FWHM (nm)
1	425.031	0.608
2	431.395	0.861
3	437.364	0.847
4	442.860	0.860
5	448.123	0.860
6	453.256	0.851

Some `n2sl` tests (standard lamp tests in the visible) were performed both during day and night, to detect any daily variation of the Brewer sensitivity owing to the instrumental temperature. According to Fig. 2, no clear temperature dependence is visible from the standard lamp. Rather, each day seems to show its own dependence. Further effort will be spent in the future to assess the influence of other factors (such as the warm-up time or the effect of the visible light entering the plastic viewing window) in order to better understand these data.

Finally, the results of the dispersion test have been analysed using an accurate fitting function (Gröbner et al., 1998) to provide the operating wavelengths and resolutions (FWHM) in the visible (grating operated at the second order) at the operative step of 985. The results are shown in Table 1. The weightings and the differential cross section, which are described further below, are calculated based on this set of wavelengths and FWMHs.

2.3 Modelling

The `libRadtran` radiative transfer model (RTM) developed by Mayer and Kylling (2005) has been employed to validate the AOD algorithm using synthetic spectra and to perform some sensitivity studies. A first script, based on this RTM, simulates the irradiance entering the Brewer optics (with or without considering diffuse light in the field of view of the instrument). Then, the AOD algorithm is applied and the extraterrestrial constants (ETCs) are calculated to match (on average at various AMFs)

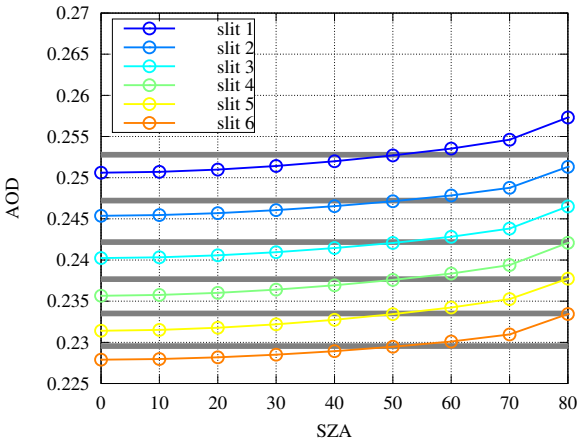

Figure 3: Retrieval of the AOD from synthetic spectra at the six Brewer operating wavelengths. The thick horizontal lines represent the AOD values given as input to the model (slightly varying as a function of the wavelength as a consequence of the Ångström law).

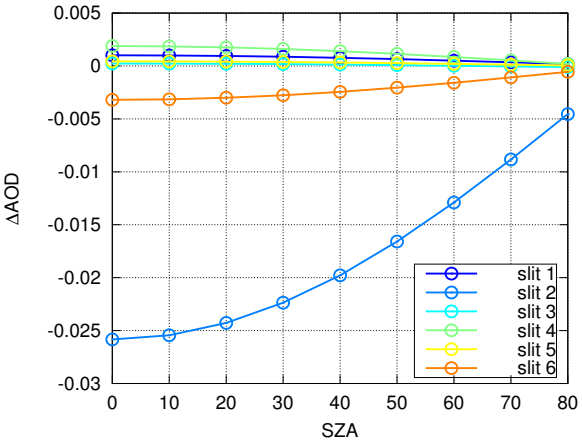

Figure 4: Simulation of the error introduced in the AOD retrieval by a misalignment of +4 micrometer steps (about 0.04 nm).

the AOD given as input to the model. Figure 3 depicts the results: the AOD values retrieved by the algorithm correspond (within the uncertainty of the method) to the input. A slight dependence on AMF is visible, probably due to the unknown profile of the aerosols in the calculation of the air mass factor, however the deviation is fully within the acceptance limits described by WMO (2004).

A second script can simulate slight systematic errors in the retrieval, such as wavelengths misalignments introduced by the measuring instrument, and is used for sensitivity studies. Figure 4 shows the error due to a misalignment of +4 micrometer steps (about 0.04 nm, not uncommon for Brewer #001), i.e. the difference between the AOD retrieved with the misalignment and without it, as a function of the solar zenith angle. As clear from the plot, and as it will often emerge later in the text, slit 2 is largely affected by wavelengths misalignments (absolute errors up to 0.025 for misalignments of 4 microsteps). The reason is due to the proximity to the border of a deep Fraunhofer line (Fig. 5), triggering large variations of the corresponding ETC when the wavelength is shifted. **As a consequence, AOD retrievals in the visible corresponding to the second slit should be used with caution**.

Finally, the sensitivity of the AOD retrieval to the diffuse light entering the field of view (FOV) of the instrument has been assessed using the model and found to be negligible for the visible (maximum differences of about $5 \cdot 10^{-4}$, not shown). The influence of this factor is much lower than in the UV due the low Rayleigh scattering in the visible range.

2.4 Historical dataset

The Cimel AOD data series measured at the 440 nm channel (actual wavelength is 438.5, changed to 439.3 in 2014 due to the replacement of the photometer) is extrapolated at the Brewer wavelengths using the Ångström exponent measured by the Cimel in the 380–500 nm range. Uncertainties associated to the Ångström exponent should not propagate considerably to the final AOD owing to the short wavelength range of the Brewer slits. This approach provides six different AOD datasets directly comparable to the Brewer, thus permitting an analysis at several wavelengths (which may provide useful information, as explained further in the text).

The analysis of the historical series is performed by employing the AERONET data at level 2.0 (i.e., cloudscreened data, quality checked and interpolated between subsequent calibrations), which ex-

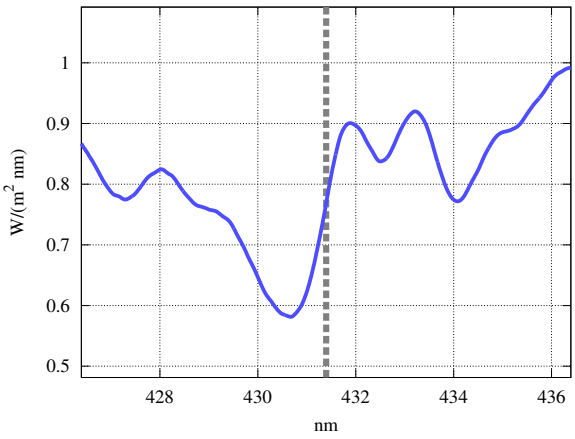

Figure 5: Simulation of direct sun irradiance spectrum (blue line) at the resolution of slit 2 and the centre wavelength of the slit (grey vertical line).

tend, however, only to the end of 2012. Only nearly simultaneous measurements (time differences lower than 1 minute between both instruments) are considered in the analysis. Taking the AOD measurements by the Cimel as reference, it is possible to assess the ETCs of the Brewer (calibration transfer). Figure 6 shows the retrieved ETCs. The instability by the Brewer is noticeable both as a large short-term scatter of the values and as long-term variations. The series of the monthly means of the ETCs, for example, exhibit a standard deviation of 0.03 (0.05 for slit 2, due to the wavelength sensitivity). In order to assess the effect of the Brewer instability on the AOD series, a median for each slit of the ETCs is taken as the reference ETC of the slit. Once the six ETCs are determined, it is possible to calculate the AOD measured by the Brewer and compare it to the Cimel. Figure 7 presents the final AOD series retrieved with the new algorithm at the third slit (at a wavelength of 437.36 nm), while Fig. 8 shows the difference between the measurements by the Brewer and the Cimel at the same wavelength. The medians of the deviations are zero, as a result of the ETC transfer from the Cimel to the Brewer. After removal of the outliers (Chauvenet criterion), the root mean square differences are about 0.03 at almost every slit (0.04 at slit 2). The histogram of the differences and the scatterplot of Cimel and Brewer measurements at slit 3

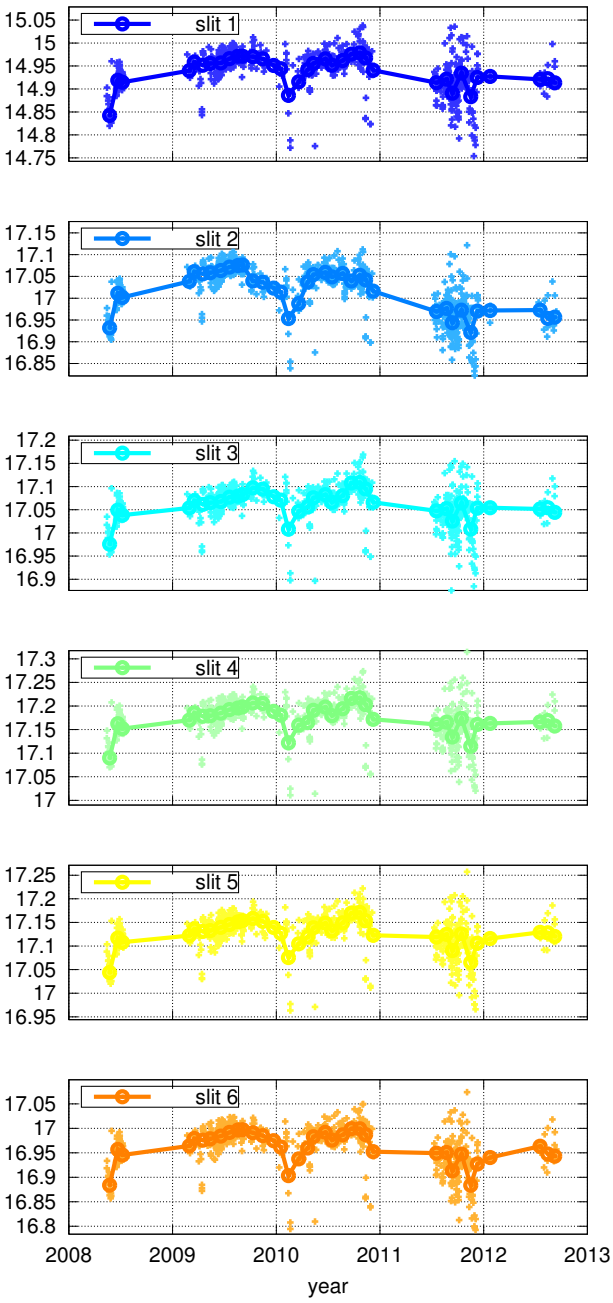

Figure 6: Extraterrestrial constants transferred from the Cimel to the Brewer at the various slits (single points) and their monthly averages (circles and lines).

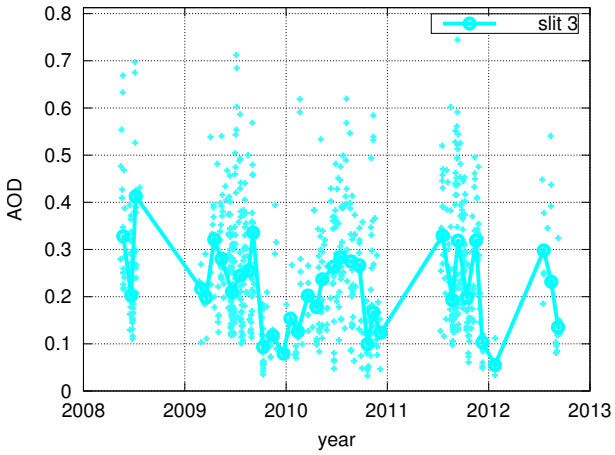

Figure 7: AOD retrieved by the Brewer at slit 3 (437.36 nm). Single values are represented by points, monthly means by circles and lines.

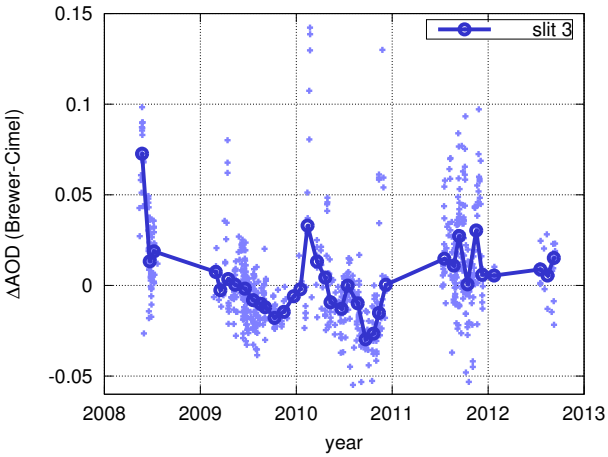

Figure 8: Difference between the AOD measured by the Brewer and the Cimel at the Brewer slit 3 (437.36 nm). Single values are represented by points, monthly means by circles and lines.

(as an example) are shown in Fig. 9 and 10 (slope of the fit: 1.006, offset: 0.003; Pearson's correlation coefficient: 0.98). A different, and somehow better, way of representing the deviations between the instruments is by plotting them against the air mass factor (AMF), as suggested by WMO (2004) and done by, e.g., Kazadzis et al. (2014), as shown in Fig. 11. Only 40% of the points (20% for slit 2) fall within the acceptance limits, while a minimum of 95% would be needed to accept the traceability between both instruments.

Finally, it can be wondered whether an approximate evaluation of the Ångström exponent can be performed in the relatively short range of about 425-453 nm of the Brewer visible measurements, although the best method would be to make use of the additional AOD measurements at the UV wavelengths, as in Gröbner and Meleti (2004). Figure 12 shows that the Brewer provides reasonable results compared to the Cimel and that the Ångström exponents without using slit 2 are less scattered than using all slits.

2.5 Principal Component Analysis (PCA)

The extrapolation of the Cimel AOD at the six Brewer wavelengths allows not only to certify the differences between the two datasets but also to understand in more depth the reason of the observed deviations using some sort of "spectral" analysis. Principal Component Analysis (PCA) of the differences between the Brewer and the Cimel AODs seems the best approach. As an input, the technique requires a matrix whose columns are the time series at the six wavelengths. As an output, it provides two matrices: the first includes six vectors representing the main "modes" of variation of

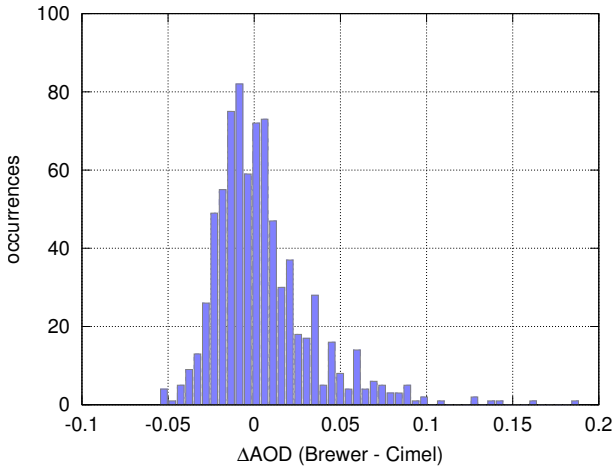

Figure 9: Histogram of the differences between the AOD measured by the Brewer and by the Cimel at the Brewer slit 3 (437.36 nm).

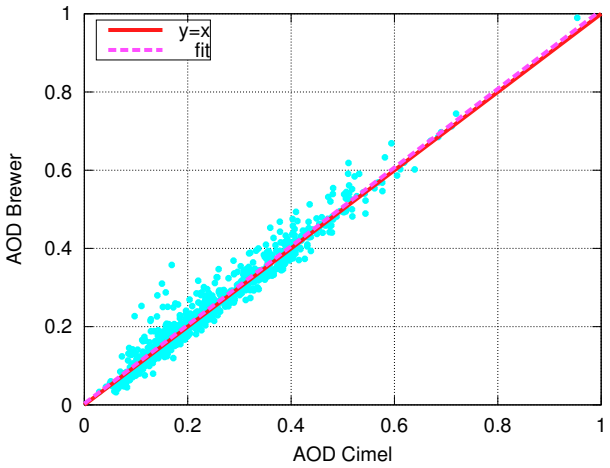

Figure 10: Scatterplot of Brewer and Cimel AOD measurements at the third slit. The red line represents the bisectrix of the first and third quadrant and the violet line the fit to the data.

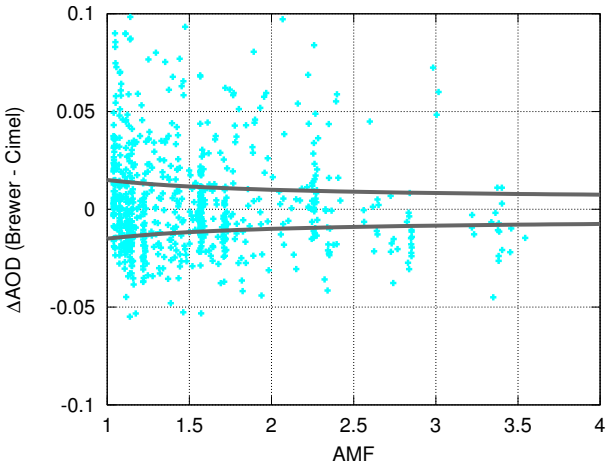

Figure 11: Difference between the AOD measured by the Brewer and by the Cimel at the Brewer slit 3 (437.36 nm) as a function of the air mass. The thick lines represent the limits defined by WMO (2004) for traceability.

the series, ordered by the variance they explain; the second contains the temporal series of weighting factors ("scores" or "principal components") for each mode. Moreover, the scores are orthogonal, i.e. the new series resulting from the analysis are statistically uncorrelated. The input dataset is thus decomposed in different modes whose linear combination can reconstruct the original series and whose spectral shapes can be compared to known factors affecting the AOD calculations. Although no rigorous conclusion can be drawn from this kind of correlation, some results seem reasonable.

The results of the PCA applied to the difference ΔAOD (AOD Brewer - AOD Cimel) are shown in Fig. 13 and can be summarised as follows:

1. the first mode explains 99.4% of the variance and is almost spectrally flat. This means that the differences between the two instruments do not relevantly depend on wavelength. However, both mode 1 and 2 (0.5% of the total variance) are connected to the wavelength shifts of the Brewer. This is confirmed by comparing the shape of the two vectors to the wavelength derivative of the logarithm of the solar spectrum. The latter was obtained using the results from a radiative transfer model. Furthermore, the second series of weightings is highly correlated to the jumps that are also observed in the NO_2 series (Diémoz, 2014), which were already proven to be connected to the wavelength misalignments;

2. the third mode is approximately linear with wavelength and could be a sum of several factors which also vary linearly with wavelength. However, it could also be correlated with the temperature dependence of the Brewer ob-

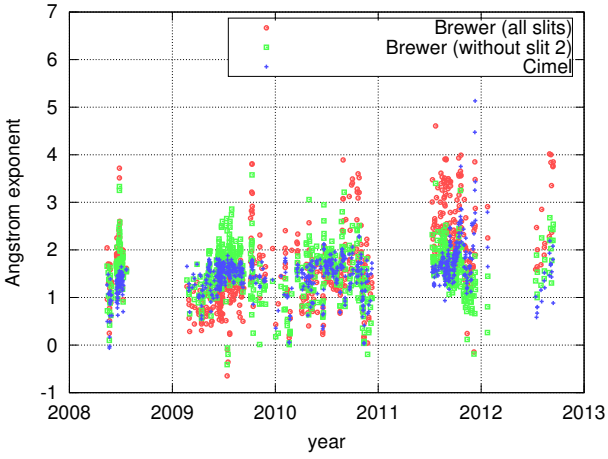

Figure 12: Ångström exponent from the Brewer (calculated with and without slit 2) and the Cimel.

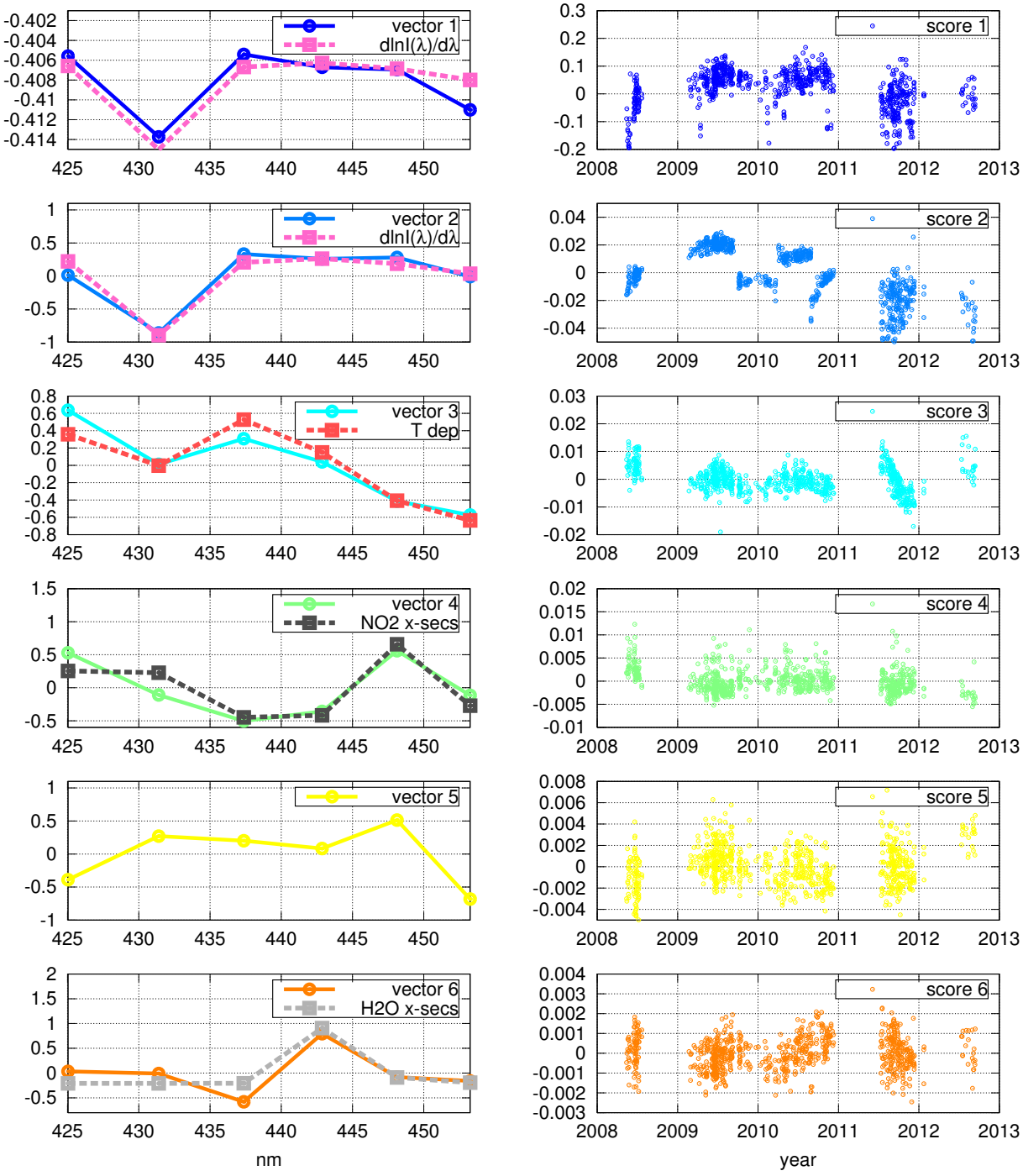

Figure 13: Results of the PCA applied to the differences of the AODs measured by the Brewer and the Cimel. The figures on the left represent the main modes of variation and the figures on the right the temporal series of the respective weights. The wavelength derivative of the logarithm of the solar spectrum is plotted together with modes 1 and 2; the temperature dependence obtained in Sect. 2.6 is plotted with mode 3; the NO_2 and H_2O cross sections at the Brewer wavelengths are plotted along with modes 4 and 6, respectively. Units along the y axes are arbitrary.

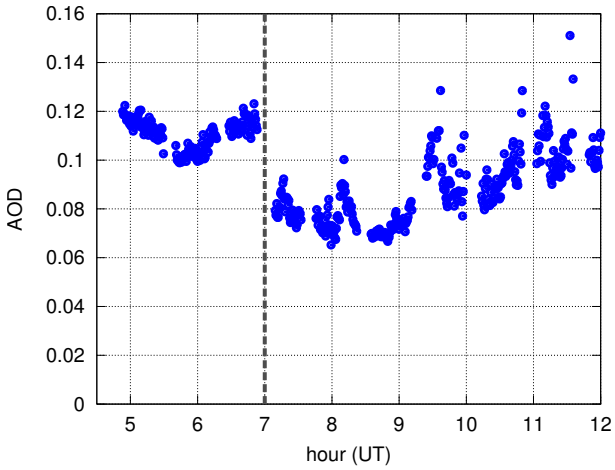

Figure 14: Effect of cleaning the quartz window (the dashed line represents the time of the cleaning).

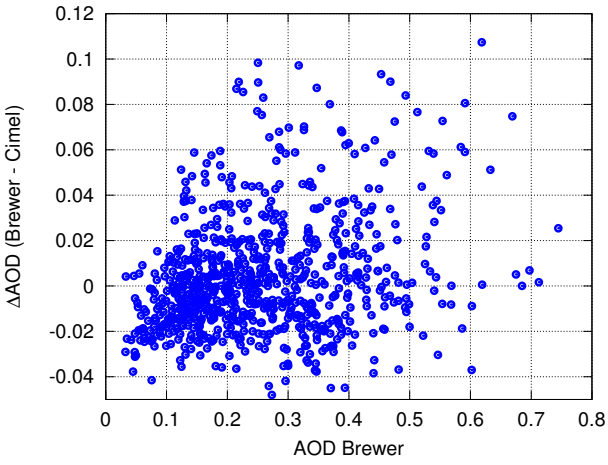

Figure 15: Differences between Brewer and Cimel datasets as a function of the AOD measured by the Brewer.

tained in Sect. 2.6. This mode explains 0.03% of the total variance of the differences;

3. the fourth mode seems to be connected to the NO_2 cross section and could denote that the NO_2 climatology used for the AERONET processing is probably not appropriate. Likely, the fifth vector also includes some residuals of the NO_2 influence. These modes represent 0.01% and 0.005% of the total variance;

4. finally, although carrying a very low variance (about 0.001%) – which indicates a low signal – the sixth vector could include some influence by the water vapour, absorbing at the fourth Brewer slit. As a further indication, the corresponding series of scores appears to correlate, although weakly, to the H_2O series recorded by the Cimel at 940 nm (not shown).

2.6 Measurements during the STSM

Some instrumental issues were identified during the first week of the STSM, which are reported here as interesting cases for the whole Brewer users community. First, the effect of some dust accumulating on the quartz window as a consequence of a Saharan dust event accompanied by some rain, is shown in Fig. 14. After cleaning the optics, the AOD apparently decrease by about 0.03, which is a rather large fraction of the total optical depth in this relatively clean day. Therefore, a first conclusion can be drawn: **if accurate AOD measurements are needed, frequent cleaning of the optics is required, especially after rain episodes**. This is likely most important for absolute measurements, as in the case of AOD, than retrievals based on ratios, as for nitrogen dioxide. Interestingly, the differences between the AOD measured by the Brewer and the Cimel in the historical series appear connected to the AOD measured by the Brewer (Fig. 15), but not to the ones measured by the Cimel (not shown), which could confirm the hypothesis that the Brewer overestimates when its optics are dirty.

A second case study is depicted in Fig. 16, when some pointing errors have occurred as a consequence of lacking synchronisation by the PC operating the Brewer. As the sun crosses the border of the iris, the AOD apparently increases. Regular checks of the sighting and levelling along with the use of the `td` routine can overcome the issue.

During the rest of the STSM, great care has been taken to guarantee accurate AOD measurements, by frequently cleaning the optics and checking the sighting. Also, a special schedule has been adopted to gather a large number of measurements. This allows to consider the short series registered in the second half of the STSM and in the following few weeks as a very accurate subset of the full series to

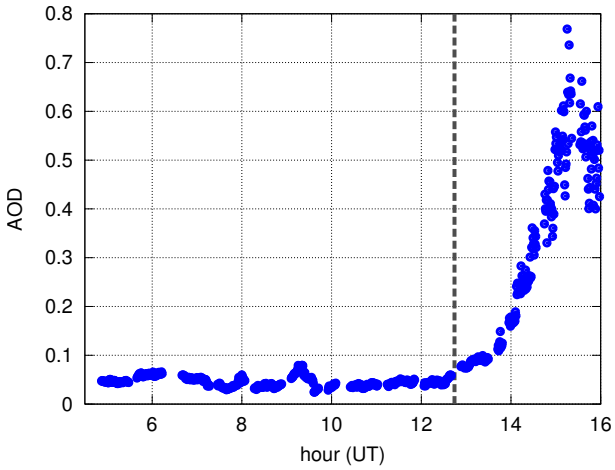

Figure 16: Effect of pointing errors and sun leaving the field of view of the instrument (the dashed line represents the time when the iris border starts cutting the sun image).

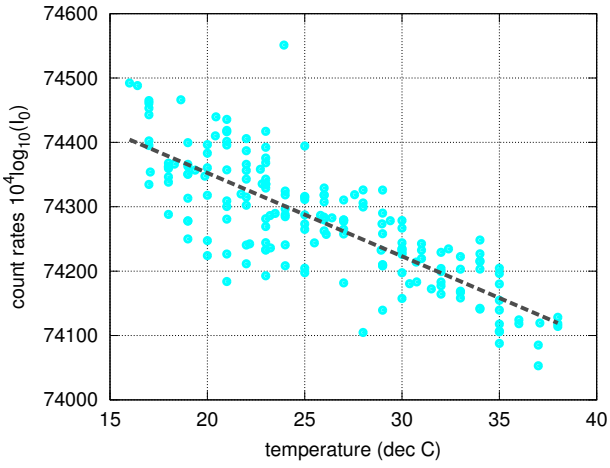

Figure 17: Temperature dependence of the transferred extraterrestrial constants for slit 3.

be compared with the Cimel.

Even though specific ETCs are calculated using only the short series, which in principle would allow a better fit of the Brewer data to the Cimel, some discrepancies between both instruments are found. Among all analysed factors, the Brewer internal temperature is the one that best correlates with the change of the transferred ETC. Figure 17 shows the correlogram between temperature and the ETC at slit 3. The slope of the fit corresponds to a rate of about -0.3%/°C, which is fully compatible with previous results reported in the scientific literature (Meltzer et al., 2000; Weatherhead et al., 2001; Taylor and Kimlin, 2002) and can be attributed to the temperature dependence of the photomultiplier tube (PMT), since the $NiSO_4$ filter is not used in the visible. This rate could be large enough to trigger a seasonal cycle up to ±6% in the course of the year, reflecting changes of the internal temperature of ±20°C. Moreover, the temperature dependence is slightly different for each wavelength, giving rise to a pattern that apparently correlates quite well with the third vector of the PCA (Fig. 13). However, some care must be taken before drawing quick conclusions, because:

1. the temperature dependence was assessed using the AERONET data from level 1.5. In the following level of processing, 2.0, the temperature coefficients of the Cimel photometer could be slightly different;

2. the measurements using the internal standard lamp do not show any definite temperature dependence (but some issues, already explained in the previous text, could account for the observed behaviour);

3. the temperature correction factors retrieved using the new series do not improve the results when applied to the historical dataset;

4. when I_0 from the historical dataset is plotted as a function of temperature, no dependence can be clearly seen. However, this could also reflect changes in the temperature dependence over the years by the Brewer.

However, if both the temperature sensitivity and its wavelength dependence are confirmed, this could represent and issue also for measurements based on ratios in the visible and should be taken into account in the NO_2 retrieval.

When the temperature correction is applied to the new Brewer series, the deviations with the Cimel vanish (Fig. 18 and 19). Obviously, a longer series with high accuracy could provide more details to the analysis. No residual dependence on the selected filter is observed, revealing a good filter characterisation in the visible range.

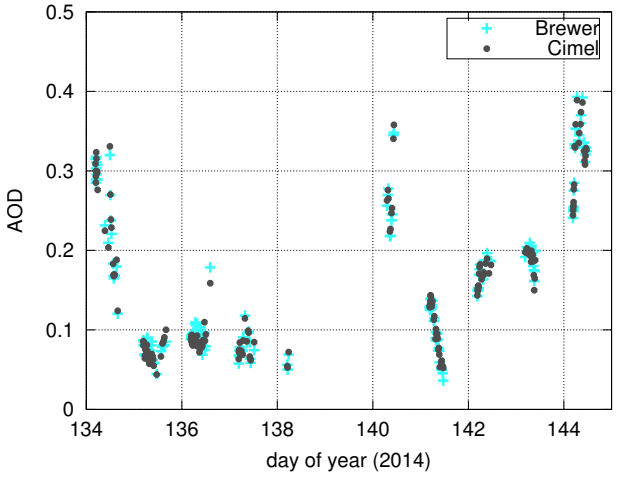

Figure 18: AOD series registered during the STSM. The Brewer series is corrected taking into account the dependence on the internal temperature.

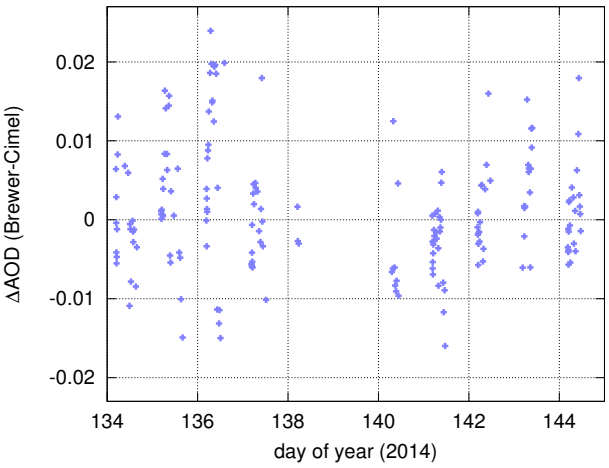

Figure 19: Differences between the Brewer and Cimel AOD series during the STSM.

3 Nitrogen dioxide (NO_2)

3.1 Algorithms

The results of the NO_2 retrieval from the Athens dataset using the original NO_2 Brewer algorithm, implemented in the Brewer operating software, are shown in Fig. 20(a). A threshold based on the standard deviation of the samples and the count rates is additionally applied to remove clouds from the measurements. High values can generally be observed owing to the use of obsolete cross sections and other issues explained in more detailed by Diémoz et al. (2014). Also, the values retrieved by the standard algorithm are quantised, as a result of a numerical truncation to the first decimal digit by the Brewer operational software. Figure 20(b) shows the results using the algorithm developed by Diémoz (2014), including several improvements. As an example, lower estimates – approaching to the values measured by other instruments and the satellites – are obtained by employing the most recent laboratory cross sections. However, the algorithm is still sensitive to slight wavelength misalignments and several "jumps" can be noticed in the series corresponding to some micrometer adjustments. For this reason, the bootstrap method (Herman et al., 2009) was applied on each portion of the series and the baseline is much more stable (Fig. 20(c)). Unfortunately, the last method also removes any seasonal cycle or long-term trend in the baseline.

The algorithm has been thus improved during the STSM. Together with the Rayleigh scattering cross section by Bodhaine et al. (1999), the Mie extinction (proportional to λ^{-1}) and a spectrally constant term, the wavelength derivative of the logarithm of the solar spectrum (Fig. 13, plots of the first and second vectors) has also been included in the fit instead of the ozone cross section (since the O_3 cross section is very low and smooth in the MKIV measurement range, its effect is expected to be negligible). This makes the fit much less sensitive to the measuring wavelengths, since the additional term "absorbs" the error induced by slight micrometer misalignments on the NO_2 retrieval. An explanation (which cannot be described in detail in this short report) can be obtained by applying a Taylor expansion to the Brewer equation and focussing on the term

$$\frac{\partial \log I(\lambda)}{\partial \lambda} = \frac{\partial \log I_0(\lambda)}{\partial \lambda} + \mu_{NO_2} X_{NO_2} \frac{\partial \sigma_{NO_2}}{\partial \lambda} \quad (1)$$

the first term on the right side represents the contribution from the wavelength variability of the extraterrestrial spectrum, which can be proven to introduce an offset in the NO_2 retrieval (dependent on the AMF). This is the main factor triggering the steep variations observed in Fig. 20(b). The sec-

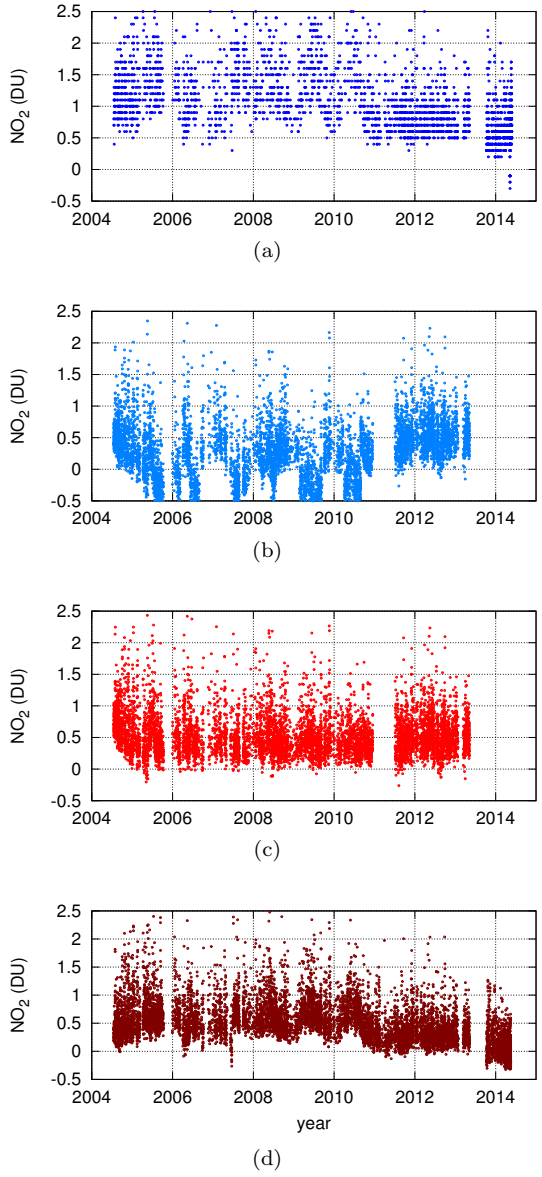

Figure 20: Results of NO_2 retrievals from the same Athens series using four different algorithms: `(a)` standard algorithm from Brewer processing software; `(b)` new algorithm by Diémoz (2014); `(c)` same as `(b)`, but with further processing to remove the jumps of the NO_2 baseline ("piecewise" calibration); `(d)` new algorithm developed during the STSM (no ETC correction is applied, yet).

Table 2: Weighting factors used for the linear combination of the logarithms of the solar irradiances at the various slits in the NO_2 algorithm developed during the STSM.

slit	γ_i
1	0.07
2	0.04
3	-0.28
4	-0.24
5	0.83
6	-0.41

ond term comes from the wavelength variability of the nitrogen dioxide cross section and can potentially introduce a scale factor in the NO_2 retrieval. However, several RTM simulations performed during the STSM, using a wide range of NO_2 input values, demonstrate that the quantity at the left side of the equation does not considerably depend on the NO_2 VCD, since the most important contribution comes from the first term. This legitimates the use of a constant vector in the retrieval algorithm. Finally, several ET spectra have been tried, but they provide similar results.

The new weighting factors used in the NO_2 retrieval are reported in Table 2. The low magnitude of the second weighting "tells" the algorithm to mostly ignore the results from slit 2, which are more affected by wavelength inaccuracies.

3.2 Modelling

Radiative Transfer Models (RTMs) have been used to validate the new algorithm, by comparing the NO_2 VCD given as input to the model and the retrieval from the synthetic spectra. Results agree within 0.02 DU and mainly depend on the parameterisation of the AMF (not shown).

Additionally, RTMs are used to assess the sensitivity of the retrieval to many factors:

1. the measurement noise in the STSM algorithm is comparable to the noise of the algorithm by Diémoz (2014);

2. the sensitivity to the oxygen dimer (O_4) has not increased and can be corrected, as before,

using radiative transfer models (not done in this work, yet);

3. the new algorithm is a bit more sensitive to H_2O (-0.07 DU for a completely saturated atmosphere, whereas it was 0.02 DU for the previous algorithm);

4. the Ring effect (for zenith sky measurements) is also greatly reduced (by a factor 10), as a consequence of the lower importance to the measurements through slit 2, close to a deep Fraunhofer line;

5. the O_3 sensitivity, which was minimised in the previous algorithm including the ozone cross section in the fit, has slightly increased (-0.03 DU for an ozone SCD of 680 DU). However, this contribution can be easily corrected by knowing the O_3 VCD measured in the UV range. Futher efforts will be spent in the future in order to assess the beneficial effects of additionally including the ozone cross section in the fit (indeed, the algorithm has one remaining degree of freedom) and evaluate whether the measurement noise increases or not.

3.3 Results

The extraterrestrial constant is determined using the bootstrap method over the period 2008–2010, which seems reasonably stable. Figure 20(d) shows the results by applying the method developed during the STSM. No ETC correction based on the results of the `n2sl` tests has been applied, yet. The baseline appears to be much smoother than in Fig. 20(b). However, the seasonality from the retrieval (minimum in winter and maximum in summer) is opposite than expected for a polluted site (maximum in winter and minimum in summer). Also, some instabilities are visible in the course of the series (e.g., negative values in 2014). Future work will focus on these issues, which are still not fully understood.

3.4 Comparison with in-situ NO_2 concentrations

The Brewer estimates of the NO_2 VCD have been compared to nearly-simultaneous ($\Delta t < 1$ hour) in situ measurements of tropospheric nitrogen dioxide concentration. Indeed, in a polluted site, the total column should be driven, in principle, by the tropospheric contribution. The correlation index between the Brewer estimates and the measurements performed at the Marousi station is highly variable from one year to the other (e.g., 0.59 in 2008 and 0.11 in 2009), while the correlation index for the Nea Smyrni station seems more stable, with values of about 0.5 and a maximum of 0.59. These indexes are higher than the ones found by Diémoz (2014), of about 0.4, likely reflecting a slight improvement of the Brewer retrieval algorithm.

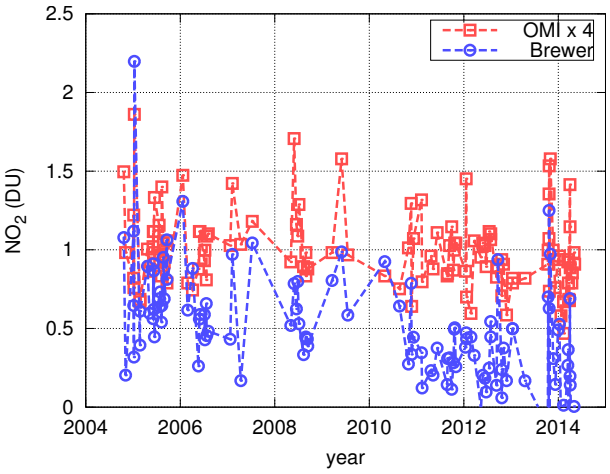

Figure 21: Nearly-simultaneous measurements by the Brewer and OMI. It should be noted that OMI data had to be multiplied by 4 to approximately match the Brewer estimates (see text).

3.5 Comparison with spaceborne radiometers

In previous studies, the Brewer NO_2 measurements have been compared to the monthly estimates over Athens from three satellite radiometers (OMI, SCIAMACHY and GOME-2), processed by the Institute of Environmental Physics (IUP), University of Bremen (e.g., Hilboll et al., 2013). While the average values of both series agreed, with maximum biases of -0.04 DU, the short-term correlation was rather low (from 0.09 to 0.36 depending on the satellite). It was therefore decided to analyse the daily overpass data to understand the issue in more depth. However, since the requested satellite

data were not processed soon enough for the STSM, the TEMIS overpass data, freely available on the web (`http://www.temis.nl/airpollution/no2col/overpass_no2.html`), were used instead of the ones from IUP.

The comparison was performed by filtering the satellite data based on both their distance from the station and the retrieved cloud fraction in the satellite pixel. The maximum allowed distance is 15 km for OMI, 30 km for SCIAMACHY and 50 km for GOME-2. The maximum cloud fraction is 0.1 for OMI and SCIAMACHY and 0.2 for GOME-2. The limits were arbitrary chosen to obtain a reasonable number of points in the comparison: 119 using OMI, 57 for SCIAMACHY and 161 for GOME-2.

The correlation using the TEMIS overpass data is rather good, with Pearson's indexes of about 0.6. Figure 21 shows the series of nearly-simultaneous measurements by the Brewer and OMI. Point-to-point agreement is visible since "peaks" and "valleys" in both series generally match. However, the seasonality of the NO_2 total column retrieved by TEMIS (maximum in summer) is opposite to the one observed in the IUP monthly data (maximum in winter). Also, the magnitude of the VCDs by TEMIS is about four times lower than that from the Brewer and from IUP. These issues deserve without any doubt further investigations.

4 Conclusions

An updated method to accurately retrieve the AOD at about 440 nm from the Brewer – and comprehensive of all known factors affecting the estimates – has been developed. The relevant subroutines are made available to the community and can be used as a programming basis by the interested Brewer users (especially, MKIV owners). The algorithm has been validated using synthetic spectra calculated by a radiative transfer model (RTM). Some dependence was found from the AMF due to the parameterisation of the air mass itself. The RTM has also allowed to discover a large wavelength dependence of the irradiance registered at the second slit. The calibration (extraterrestrial constants for each slit) has been transferred from the Cimel to the Brewer. Then, the AOD from AERONET (level 2.0) and the Brewer has been compared. The results show negligible bias (as a consequence of the calibration transfer) and root mean square differences of 0.03. However, traceability between the two instruments could not be established with reference to the WMO guidelines, only 40% of the Brewer-Cimel deviations being within the thresholds. A spectral technique (Principal Component Analysis) has been applied to the Brewer-Cimel AOD differences and reveals some patterns that can be connected to known factors, such as the wavelength and instrumental temperature dependence, the absorption by NO_2 and H_2O. During the STSM, some instrumental issues have been faced (effect of dirty optics and wrong pointing) and are described as interesting case studies. A short series of very accurate measurements has been taken during the STSM and deviations lower than ± 0.02 are found compared to the Cimel. The temperature dependence by the Brewer has been investigated by both using results from the internal standard lamp and comparing the AOD estimates from the Cimel. In the former case, no dependence was clearly found, but further work is required to remove interferences from other factors. In the latter case, a clear relationship with the instrumental temperature emerges, with a wavelength dependence that resembles one of the main modes of variations found by the PCA. However, when applied to the historical series, the correction does not improve the comparison. Further work is needed on this issue, too.

As for the nitrogen dioxide retrieval, the algorithm by Diémoz (2014) has been further improved by fitting a new vector (the wavelength derivative of the logarithm of the solar spectrum) which remarkably reduces the sensitivity to slight misalignments without considerably increasing the influence by other factors. Radiative transfer calculations have been performed to validate the algorithm and for sensitivity studies. Comparisons of the Brewer NO_2 estimates to both in situ concentrations and satellite nearly-simultaneous measurements (overpass data, filtered by pixel distance and cloud cover) give better results than before, with correlation indexes up to 0.6 in both cases. Although this results reveal an improvement of the used method, several issues are still to be investigated: the seasonality of both the Brewer and TEMIS estimates is opposite than the one expected for a polluted site; ETC corrections to the Brewer measurements based on the `sl` test results must

still be performed; the effect of the instrumental temperature and the effective nitrogen dioxide temperature must be assessed.

Finally, the STSM has been a great experience to meet scientists and make new acquaintances (Prof. Zerefos, Dr. Kazadsis and Panos Raptis, besides my host, Dr. Eleftheratos), which will be certainly maintained in the future. The writing of a poster for the Mediterranean City Conference 2014, about the recent improvements of the NO_2 Brewer retrieval, is scheduled for the next weeks. Also, a paper about the reanalysis of the NO_2 data and the comparison with satellite estimates will be written once all known issues related to the retrieval will be solved.

I would like to gratefully acknowlege the EUBREWNET COST Action for the financial support and to sincerely thank the personnel of the Academy of Athens for the hospitality and assistance.

References

Bodhaine, B. A., Wood, N. B., Dutton, E. G., and Slusser, J. R.: On Rayleigh optical depth calculations, J. Atmos. Ocean. Tech., 16, 1854–1861, 1999.

Bouguer, P.: Essai d'optique sur la gradation de la lumière, 1729.

Cede, A., Kazadzis, S., Kowalewski, M., Bais, A., Kouremeti, N., Blumthaler, M., and Herman, J.: Correction of direct irradiance measurements of Brewer spectrophotometers due to the effect of internal polarization, Geophys. Res. Lett., 33, 2006.

Cheymol, A. and De Backer, H.: Retrieval of the aerosol optical depth in the UV-B at Uccle from Brewer ozone measurements over a long time period 1984–2002, J. Geophys. Res., 108, 2003.

Diémoz, H.: Improvements to the nitrogen dioxide observations by means of the MKIV Brewer spectrophotometer, Ph.D. thesis, Sapienza – University of Rome, 2014.

Diémoz, H., Siani, A., Savastiouk, V., Redondas, A., Eleftheratos, K., Zerefos, C., Vrekoussis, M., Casale, G., Stanek, M., Burrows, J., A., R., and Hilboll, A.: Improvements to the nitrogen dioxide observations by means of the MKIV Brewer spectrophotometer, in: 14th WMO-GAW Brewer Users Group Meeting, 24-28 March 2014 Tenerife (ES), 2014.

Estellés, V., Campanelli, M., Smyth, T., Utrillas, M., and Martínez-Lozano, J.: Evaluation of the new ESR network software for the retrieval of direct sun products from CIMEL CE318 and PREDE POM01 sun-sky radiometers, Atmos. Chem. Phys., 12, 11 619–11 630, 2012.

Gröbner, J. and Meleti, C.: Aerosol optical depth in the UVB and visible wavelength range from Brewer spectrophotometer direct irradiance measurements: 1991–2002, J. Geophys. Res., 109, 2004.

Gröbner, J., Wardle, D. I., McElroy, C. T., and Kerr, J. B.: Investigation of the wavelength accuracy of Brewer spectrophotometers, Appl. Optics, 37, 8352–8360, 1998.

Herman, J., Cede, A., Spinei, E., Mount, G., Tzortziou, M., and Abuhassan, N.: NO2 column amounts from ground-based Pandora and MF-DOAS spectrometers using the direct-sun DOAS technique: Intercomparisons and application to OMI validation, J. Geophys. Res., 114, 2009.

Hilboll, A., Richter, A., and Burrows, J. P.: Long-term changes of tropospheric NO2 over megacities derived from multiple satellite instruments, Atmos. Chem. Phys., 13, 4145–4169, 2013.

Holben, B., Eck, T., Slutsker, I., Tanre, D., Buis, J., Setzer, A., Vermote, E., Reagan, J., Kaufman, Y., Nakajima, T., et al.: AERONET – A federated instrument network and data archive for aerosol characterization, Remote Sens. Environ., 66, 1–16, 1998.

Kasten, F. and Young, A. T.: Revised optical air mass tables and approximation formula, Appl. optics, 28, 4735–4738, 1989.

Kazadzis, S., Veselovskii, I., Amiridis, V., Gröbner, J., Suvorina, A., Nyeki, S., Gerasopoulos, E., Kouremeti, N., Taylor, M., Tsekeri, A., and Wehrli, C.: Aerosol microphysical retrievals from Precision Filter Radiometer direct solar radiation measurements and comparison with AERONET,

Atmos. Meas. Tech. Discuss., 7, 99–130, doi: 10.5194/amtd-7-99-2014, 2014.

Mayer, B. and Kylling, A.: Technical note: The libRadtran software package for radiative transfer calculations - description and examples of use, Atmos. Chem. Phys., 5, 1855–1877, 2005.

Meltzer, R., Wilson, A., Kohn, B., and Rives, J.: Temperature dependence of the spectral response for the MKIV Brewers in the UGA/USEPA network, in: 6th Brewer Workshop, Tokyo, Japan, vol. 10, p. 12, 2000.

Michalsky, J. J.: The Astronomical Almanac's algorithm for approximate solar position (1950–2050), Sol. Energy, 40, 227–235, 1988.

Smirnov, A., Holben, B., Eck, T., Dubovik, O., and Slutsker, I.: Cloud-screening and quality control algorithms for the AERONET database, Remote Sens. Environ., 73, 337–349, 2000.

Taylor, T. and Kimlin, M.: Temperature dependence of the Brewer spectrophotometer, Tech. rep., National Ultraviolet Monitoring Center, 2002.

Vrekoussis, M., Richter, A., Hilboll, A., Burrows, J., Gerasopoulos, E., Lelieveld, J., Barrie, L., Zerefos, C., and Mihalopoulos, N.: Economic crisis detected from space: Air quality observations over Athens/Greece, Geophys. Res. Lett., 2013.

Weatherhead, E., Theisen, D., Stevermer, A., Enagonio, J., Rabinovitch, B., Disterhoft, P., Lantz, K., Meltzer, R., Sabburg, J., DeLuisi, J., et al.: Temperature dependence of the Brewer ultraviolet data, J. Geophys. Res., 106, 34 121–34 129, 2001.

WMO: WMO/GAW experts workshop on a global surface-based network for long term observations of column aerosol optical properties, Tech. rep., WMO/GAW, 2004.